AD-A159 400 SIMULATION OF TURBULENT BOUNDARY LAYER WALL PRESSURE FLUCTUATIONS(U) OLD DOMINION UNIV NORFOLK VA DEPT OF MECHANICAL ENGINEERING AND MECHANICS R L ASH ET AL. 1/1

UNCLASSIFIED AUG 85 N00014-82-K-0639 F/G 20/4 NL

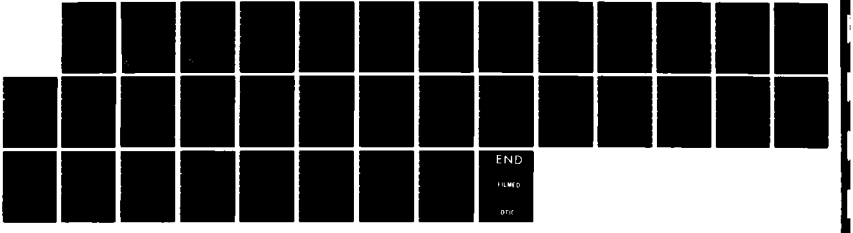

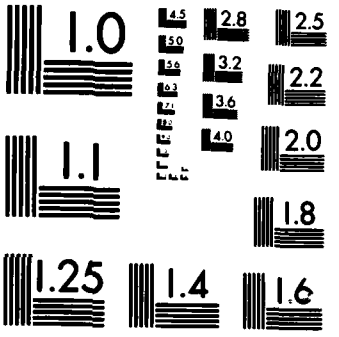

(2)

DEPARTMENT OF MECHANICAL ENGINEERING AND MECHANICS
SCHOOL OF ENGINEERING
OLD DOMINION UNIVERSITY
NORFOLK, VIRGINIA

SIMULATION OF TURBULENT BOUNDARY LAYER WALL PRESSURE FLUCTUATIONS

By

Robert L. Ash, Principal Investigator

and

Mehdi R. Khorrami

Final Report
For the period ending September 30, 1984

Prepared for the
Department of the Navy
Office of Naval Research
800 N. Quincy Street
Arlington, Virginia 22217

Under
Research Grant N00014-82-K-0639
Task No. NR 657-694
Dr. M. M. Reischman, ONR Scientific Officer

August 1985

DEPARTMENT OF MECHANICAL ENGINEERING AND MECHANICS
SCHOOL OF ENGINEERING
OLD DOMINION UNIVERSITY
NORFOLK, VIRGINIA

SIMULATION OF TURBULENT BOUNDARY LAYER WALL PRESSURE FLUCTUATIONS

By

Robert L. Ash, Principal Investigator

and

Mehdi R. Khorrami

Final Report
For the period ending September 30, 1984

Prepared for the
Department of the Navy
Office of Naval Research
800 N. Quincy Street
Arlington, Virginia 22217

Under
Research Grant N00014-82-K-0639
Task No. NR 657-694
Dr. M. M. Reischman, ONR Scientific Officer

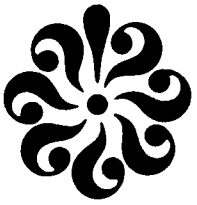

Submitted by the
Old Dominion University Research Foundation
P. O. Box 6369
Norfolk, Virginia 23508

August 1985

Unclassified

SECURITY CLASSIFICATION OF THIS PAGE *(When Data Entered)*

REPORT DOCUMENTATION PAGE		READ INSTRUCTIONS BEFORE COMPLETING FORM
1. REPORT NUMBER 1	2. GOVT ACCESSION NO. AD-A159 400	3. RECIPIENT'S CATALOG NUMBER
4. TITLE *(and Subtitle)* Simulation of Turbulent Boundary Layer Wall Pressure Fluctuations		5. TYPE OF REPORT & PERIOD COVERED FINAL July 1, 1983 - Sept. 30, 1984 6. PERFORMING ORG. REPORT NUMBER
7. AUTHOR(s) Robert L. Ash, Principal Investigator Mehdi R. Khorrami		8. CONTRACT OR GRANT NUMBER(s) N000014-82-K-0639
9. PERFORMING ORGANIZATION NAME AND ADDRESS Department of Mechanical Engineering & Mechanics Old Dominion University Norfolk, University 23508		10. PROGRAM ELEMENT, PROJECT, TASK AREA & WORK UNIT NUMBERS Mechanics Division NR 657-694
11. CONTROLLING OFFICE NAME AND ADDRESS ONR Resident Representative Joseph Henry Building Rm 623 2100 Pennsylvania Ave., N.W. Washington, DC 20037		12. REPORT DATE ~~June~~ Aug 1985 13. NUMBER OF PAGES
14. MONITORING AGENCY NAME & ADDRESS*(if different from Controlling Office)*		15. SECURITY CLASS. *(of this report)* Unclassified 15a. DECLASSIFICATION/DOWNGRADING SCHEDULE

16. DISTRIBUTION STATEMENT *(of this Report)*

This document has been approved for public release; its distribution is unlimited.

17. DISTRIBUTION STATEMENT *(of the abstract entered in Block 20, if different from Report)*

18. SUPPLEMENTARY NOTES

19. KEY WORDS *(Continue on reverse side if necessary and identify by block number)*

20. ABSTRACT *(Continue on reverse side if necessary and identify by block number)*

A Monte Carlo simulation of an unsteady, two-dimensional wall pressure field has been developed. The simulation has been evaluated in terms of the statistical properties measured in a variety of turbulent boundary layer experiments and the results are generally in good agreement. Since identical pressure histories can be created using simulations, it has been possible to investigate the influence of receiver area or microphone size on the statistical measurements of identical pressure histories. The simulation has shown that only a few

DD FORM 1 JAN 73 1473 EDITION OF 1 NOV 65 IS OBSOLETE
S/N 0102-LF-014-6601

Unclassified
SECURITY CLASSIFICATION OF THIS PAGE *(When Data Entered)*

statistical properties change significantly with changes in receiver area.

SIMULATION OF TURBULENT BOUNDARY LAYER WALL PRESSURE FLUCTUATIONS

By

Robert L. Ash[1] and Mehdi R. Khorrami[2]

SUMMARY

A Monte Carlo simulation of an unsteady, two-dimensional wall pressure field has been developed. The simulation has been evaluated in terms of the statistical properties measured in a variety of turbulent boundary layer experiments and the results are generally in good agreement. Since identical pressure histories can be created using simulations, it has been possible to investigate the influence of receiver area or microphone size on the statistical measurements of identical pressure histories. The simulation has shown that only a few statistical properties change significantly with changes in receiver area.

[1] Eminent Professor, Department of Mechanical Engineering and Mechanics, Old Dominion University, Norfolk, Virginia 23508.
[2] Research Assistant, Department of Mechanical Engineering and Mechanics, Old Dominion University, Norfolk, Virginia 23508.

TABLE OF CONTENTS

LIST OF TABLES

LIST OF FIGURES

LIST OF FIGURES - continued

1. INTRODUCTION

Wall pressure fluctuations produced by turbulent boundary layer flows can produce structural vibrations and noise. In order to predict surface motion details, as part of the design process, realistic wall pressure forcing function data are required which duplicate the statistical properties of turbulent flows. Ultimately, a coupled fluid-structural analysis package which employs accurate structural modelling and the Navier-Stokes equations in three-dimensions is desired (Refs. 1, 2), but that approach presently has limited resolution and is very expensive. Experimental measurements of $P(x,z,t)$ over a rectangular region, are the next best source of forcing function data for the design process, but experimental data suffer from limited resolution, expense and the need for arbitrarily resolvable measurements over a wide range of geometrical and flow conditions. A less expensive alternative is numerical simulation. A Monte Carlo wall pressure simulation has been developed and will be described here.

While nonlinear structural systems may require real time forcing function input, wall pressure data transformed into frequency-wave number space is preferred for most linear systems, (Refs. 3-7). Even then $P(x,z,t)$ data are required to develop appropriate transformation. Those data are not available in general and most structural dynamicists and acousticians have resorted to some type of statistical decomposition assumption which permits prediction of surface amplitude spectra but may not yield reliable wave number information. Attempts to incorporate more realistic turbulence models have been reported (Refs. 3, 7, 8), but uncertainty still exists concerning interpretation of wall pressure statistics (Refs. 6, 9) and there may be a limit to the validity of statistical data using experimental instruments.

Questions concerned with the low frequency end of the pressure fluctua-

tion spectrum and limiting local root-mean square pressure levels remain (Ref. 9), but there is little doubt about the generic shape of the pressure spectrum in the primary energy region or about the decreasing correlation peak with separation distance between spatial locations. As will be shown subsequently, the statistics produced from the synthetic pressure distribution are remarkably similar to turbulent wall pressure data. While the synthetic case does not replicate the physics, the fact that identical simulated pressure fields can be produced for a range of resolution conditions has enabled this investigation to examine the influence of spatial resolution (or "microphone" size) on the statistics. That is, an identical pressure history can be used to produce the pressure force history for different sized receivers, thereby providing an unambiguous measure of the influence of sensor size on the statistics that are measured.

Schewe (Ref. 10) has measured turbulent wall pressure fluctuations using an array of transducers of varying size. His measurements suggest that as the resolution area is increased the statistical properties of the local pressure force approach Gaussian. Much of the pressure correlation data has been summarized by Willmarth (Ref. 11) and Von Winkle et al. (Ref. 6) and the reader is referred to those reviews for additional references. In the discussion which follows, only those experimental measurements which were used in developing or testing the simulation will be cited. In addition, the previous work of the authors (Refs. 12, 13) may be helpful in developing a better understanding of the approach.

2. SIMULATION STRATEGY

The simulation program was developed as a multipurpose program to model a variety of flow and geometry conditions. The program is listed in Khorrami (Ref. 13) and is made flexible by assuming that pressure fluctuation statistics scale according to the parameters listed in Table 1. That table also contains the flow variables used in the example simulations. The simulated flow conditions were similar to the experiments of Bull (Ref. 14), but several other flow conditions have been examined subsequently (Ref. 2, 15).

The simulation record is constructed from randomly distributed, discrete pressure events. Single cycle pressure fluctuations were generated using empirically based distribution functions for spacing, time of origin, peak amplitude, and wavelength. Depending upon the frequency (wavelength), the individual events were assigned convection speeds and convected downstream across the user specified measurement locations. The force resulting from the event was computed over the specified measurement area by integration at the specified sampling times. The instantaneous pressure force was the summation of all the events that contributed to that measurement area at the prescribed time.

A symbolic representation of the pressure events that are created during a single spatial pass down a streamwise track is shown in Fig. 1. Each Δx_i is generated randomly using a distribution function developed empirically from the burst cycle data of Offen and Kline (Ref. 16). The individual event location is determined as the sum of the Δx_i's that are generated during that sweep. When the location of origin exceeds the total length of the numerical experiment, a new sweep is started. The incremental time of origin is also based on the data of Offen and Kline (Ref. 16), but

TABLE 1

SCALING INFORMATION

a. Scaling Parameters

Quantity	Scaling Parameter	Symbol
Length	Displacement thickness	δ^*
Separation length parameter	Ratio of friction and free stream velocities	u_τ/U_∞
Time	Displacement thickness/free stream velocity	δ^*/U_∞
Pressure fluctuation amplitude	Wall shear stress	τ_w

b. Scaling Relations

Root mean square pressure, $P_{rms} = 2\tau_w$.

Pressure spectrum peak frequency, $2\pi f_{peak} = 0.2\ U_\infty/\delta^*$.

c. Example Simulation Case

U_∞ = 33.5 m/sec	u_τ = 1.26 m/sec	ρ = 1.2 kg/m^3
δ^* = 5.1 mm	ν/u_τ = 11 μm	Re_Θ = 9500

the event generation times were related to a reference or datum time, rather than accumulated during the sweep. At the end of a spatial sweep, an average time interval is calculated for that sweep and the reference or datum time is increased by the average time step, before the next sweep is started. That method prevented any inadvertant frequency biasing due to unnecessary time step control. Obviously, the user specified resolution time is not connected to the simulation time and, in effect, a freely varying clock and a control clock are used simultaneously to manage tne superposition calculations.

Besides the known variation of convection speed with pressure fluctuation frequency, experimental evidence suggests that the frequency or wavelength of the event also varies as the fluctuation is convected downstream (Refs. 6, 14, and 17). A wavelength adjustment was made continuously as the event convected down stream.

A characteristic convection speed or celerity can be determined by dividing the separation distance between two measurement points by the time interval associated with the peak in the two-point correlation function. It was observed during the development phase that simulations produced convection speeds which exceeded free stream velocity when adjacent points were close together $[(x_{n+1} - x_n)/\delta^* < 2]$, even though the assigned event convection speeds were always less than $0.8U_\infty$. That effect was attributable to generation of pressure events which spanned more than one measurement location at the time of origin. When new events actually bridged two locations, an "infinite" convection speed contribution could be produced. That problem was eliminated by ramping the amplitude of the event up to the prescribed value during a short time interval (which was characteristic of

the time associated with a bursting event in the Offen and Kline (Ref. 16) study). Subsequently, the amplitude of the pressure disturbance began to decay. A schematic representation of the evolution and convection of a simulated pressure event is shown in Fig. 2.

Because of the non-linear character of both the simulation events and the statistical behavior of the turbulent pressure field, the simultaneous representation of pressure statistics (r.m.s. pressure, power spectrum and two point correlation) involved a great deal of tedious trial and error adjustments of the distribution functions. An acceptable combination of distribution functions was evolved and they are contained in the computer program which is listed in Reference (13). A flow chart describing the simulation program is shown in Figure 3.

The simulation which has just been described is designed to generate an arbitrarily resolved record, $P(x_i, t_n)$, in the streamwise direction. Since other records over the same spatial interval and time can be created simply by changing the initial random number, a set of pressure records -- say $P_m(x_i, t_n)$ -- can be produced. Depending on the length of the time record and the randomness of the random number generator, it is possible to construct a set of pressure records for spatial locations, x_i, which are statistically independent. That is,

$$\overline{P_r(x,t)P_s(x,t+\tau)} \equiv \sum_{n=1}^{N-k} P_r(x_i,t_n)\, P_s(x_j,t_n + k\Delta t)/[(N-k)P_{r_{rms}} P_{s_{rms}}] \approx 0 \quad (1)$$

for all combinations of r, s, i, j and k, except r = s. Here, N is the total number of time steps, and we require that $0 \leq k \leq N/2$. As N is increased, the correlations should approach zero. The ability to produce a set of statistically independent simulation records is required to construct

a complete $P(x, z, t)$ simulation.

A. Simulation of $P(x, z, t)$

If the pressure field is to be resolved at uniformly spaced locations, z_j, in the spanwise direction, there is some distance, L_z, in which the correlation between spanwise pressure records is important. From the standpoint of the simulation, the specified length of the time record controls the deviation of the correlations in Eq. (1). A numerical scatter in the correlations is present for finite records and that scatter is used as a basis for delineating the correlation, width, L_z. That is, if

$$\overline{P_r(x, t)\, P_s(\bar{x}, t + \tau)} \leq \epsilon \tag{2}$$

for time records of length $N\Delta t$, then there is a corresponding interval, L_z, such that

$$\overline{P(x, z, t)\, P(x, z + \Delta z_m, t + \tau)} \geq \epsilon, \tag{3}$$

for Δz_m less than or equaL to L_z.

The experimental data of Bull (Ref. 14) and Willmarth and Wooldridge (Ref. 17) can be used to estimate the interval over which a spanwise correlation is greater than or equal to ϵ.

For a spanwise spacing of Δz, there are N_z statistically connected pressure simulation tracks,

$$P_n(x_i, t_n), P_{n+i}(x_i, t_n), \ldots . P_{n+N_z}(x_i, t_n),$$

where N_z is the integer value of

$$N_z = (L_z/\Delta z) + 0.99. \tag{4}$$

This control requirement becomes quite involved for a rectangular area which is wide compared to Δz, since the correlations must be controlled for all adjacent simulation tracks in both lateral directions. The correlations can be generated by constructing $P(x_i, z_j, t_n)$ from more than one simulation track. That is, we can let

$$P(x_i, z_j, t_n) = \sum_{M=1}^{Nz} a_M P_{j+M-1}(x_i, t_n), \tag{5}$$

where

$$\sum_{M=1}^{Nz} a_M^2 = 1, \tag{6}$$

and

$$\begin{aligned} a_1 a_2 + a_2 a_3 + \ldots + a_{N_z - 1} + a_{n_z} &= R_1 \\ a_1 a_3 + a_2 a_4 + \ldots + a_{N_z - 2} a_{N_z} &= R_2 \\ a_1 a_{N_z} &= R_{N_z - 1}, \end{aligned} \tag{7}$$

The values of $R_1, R_2 \ldots R_{N_z - 1}$ are specified from the experimental spanwise correlation data (Ref. 14, 17) for separation distances of $\Delta z/\delta^*$, $2\Delta z/\delta^*$, etc. The values of the coefficients, a_M, must be determined by trial and error. It follows that

$$P(x_i, z_1, t_n) = a_1 P_1(x_i, t_n) + a_2 P_2(x_i, t_n) + \ldots + a_{N_z} P_{N_z}(x_1, t_n),$$

$$P(x_i, z_2, t_n) = a_1 P_2(x_i, t_n) + a_2 P_2(x_i, t_n) + \ldots$$

$$+ a_{N_z} P_{N_z + 1}(x_i, t_n), \quad \text{etc.} \tag{8}$$

An example simulation has been described previously (Ref. 12) where a spanwise separation distance of 2.5 δ^* was used and the time record (4000 data points per station) was such that a scatter of approximately 10 percent was observed in the uncontrolled correlation functions ($\varepsilon = 0.10$). Under those conditions the correlations at 2.5 δ^* and 5 δ^* were controlled, while correlations for larger distances were uncontrolled and, therefore, scattered about ±0.10. Variation in correlations from the simulation are shown in Fig. 4, along with a nominal fit of the experimental data for $\tau = 0$ (Ref. 14, 17).

3. RESULTS AND DISCUSSION

A typical segment of simulated pressure is shown in Fig. 5 for three locations over the same time interval. For small separation distances ($\Delta x^+ = 770$ or $\Delta x/\delta^* = 1.7$), the pressure histories are similar, but at $\Delta x^+ = 6100$, little similarity remains. The receiver "diameter" was $u_\tau\, d/\nu = 36$ or $d/\delta^* = 0.08$[1]. Schewe (Ref. 10) has shown similar data for actual turbulent wall pressure measurements.

It is also interesting to observe the influence of the receiver area on the recorded signal driven by an identical pressure field. The pressure histories generated on a receiver area (at x=o) which is half as large as the one in Figure 5 (i.e., $d^+ = 18$) and for one which is more than an order of magnitude larger ($d^+ = 270$) are shown in Figure 6. The reference case ($d^+ = 36$) is also shown. While the records for the two small receivers are very similar, it is obvious that the large receiver area results in an integrated force per unit area record which is very different.

The characteristic dimension of the pressure receivers can be changed simply by changing a line of computer code. By subjecting different sensing areas to the same pressure history, the influence of receiver size on root mean square pressure can be studied. For $u_\tau\, d/\nu > 400$, spanwise decorrelation must be considered, but with that effect neglected, r.m.s. pressure is shown as a function of receiver size in Fig. 7. Those data appear to agree with the measurements of Bull and Thomas (Ref. 18) in terms of the increase in r.m.s. pressure with decreasing transducer size. However, the diameter effect starts at a much smaller value of $u_\tau d/\nu$ than any of the experimental measurements.

---

[1] For a characteristic sensing area dimension, $d/\delta^* < 1$, the spanwise correlation measurements are sufficiently close to unity to ignore spanwise effects. Then the streamwise length is equivalent to a diameter.

Wall pressure energy spectra are shown for three different receiver areas in Fig. 8 along with a cross hatched composite of experimental measurements. The peak frequency becomes delineated more clearly as the sensing area becomes smaller, and there is a slight increase in high frequency energy. However, overall shape of the power spectrum is not sensitive to receiver area.

Variation of streamwise two point correlation functions with receiver size and separation distance are shown in Fig. 9. It is interesting to note that the correlations spread and diminish as the receiver size is decreased. This effect is due to the inclusion of small scale pressure fluctuations which decay more rapidly and thus decorrelate adjacent pressure signals. A slight irregularity in the correlations for the smallest receiver area is due to the prescribed time step resolution and should be ignored.

Because of the way in which the simulation was produced it was easy to employ a pseudo-filter and examine the streamwise correlations. If a random event had a frequency of interest, it was allowed to contribute to the wall pressure data. If it did not have a frequency of interest, it was ignored. Thus, two point correlations could be developed which consisted of only those events containing prescribed frequencies. High and low frequency correlations are shown for a range of separation distances in Figs. 10 and 11 along with the experimental measurements of Willmarth and Wooldridge (Ref. 17). Since single cycle events carry side band frequencies, in addition to their prescribed frequencies, this filtering technique is not perfect.

Schewe (Ref. 10) examined the influence of receiver size on the skewness and flatness of the wall pressure fluctuation signal. A comparison between his measurements and the simulation data are shown in Figs. 12 and

13. While the skewness data agree that there is a higher probability for negative pressure fluctuations as the receiver area decreases, there is a significant discrepancy between the flatness or kurtosis of the simulation and Schewe's measurements.

4. CONCLUSIONS

A Monte Carlo based simulation has been developed which can produce simulated turbulent wall pressure fields. The statistics generated from the simulations are in reasonably good agreement with experimental measurements and since the simulated field can be replicated for different receiver dimensions, it was possible to compare statistical properties for systems subjected to identical pressure fields.

Based on these simulations, it was possible to conclude that the root mean square pressure levels increase in a quasi linear manner as the receiver size ("microphone") decreases. The trend is in substantial agreement with the experiments of Bull and Thomas (Ref. 13), but the threshold of the diameter effect and the magnitude of the r.m.s. increase may be controlled by flow phenomena that are either ignored or improperly simulated. The power spectra are nearly insensitive to receiver size in the energy containing frequency interval. Two-point correlations first show higher correlations with decreasing receiver size, then show poorer correlations as the receiver size becomes small enough to sense fine scale phenomena.

The authors believe this simulation program can be a valuable tool in studying the response of complex or non-linear structures to quasi-random wall pressure fields. The ability to adjust resolution and simulated flow conditions arbitrarily make this a flexible tool in the analysis and design of fluid-structural systems.

REFERENCES

1. Bakewell, H.P. Jr., and W.A. Von Winkle, "Hydrodynamic Noise and Surface Compliance--An Overview of the Naval Underwater Systems Center IR/IED Program," Presented at the 109th meeting of the Acoustical Society of America, Austin, Texas, April 1985.

2. Buckingham, A.C., M.S. Hall, and R.C. Chun, "Numerical Simulations of Compliant Material Response to Turbulent Flow," AIAA Journal, Vol. 23, pp 1046-1052, 1985.

3. Maestrello, L., "Use of Turbulent Model to Calculate the Vibration and Radiation Responses of a Panel, with Practical Suggestions for Reducing Sound Level," J. Sound Vibr., Vol. 5, pp 407-448, 1967.

4. Blake, W.K., and D.M. Chase, "Wavenumber-Frequency Spectra of Turbulent-Boundary-Layer Pressure Measured by Microphone Arrays," J. Acoust. Soc. Am., Vol. 49, pp 862-877, 1971.

5. Aupperle, F.A., and R.F. Lambert, "On the Utilization of a Flexible Beam as a Spatial Filter," J. Sound Vibr., Vol. 24, pp 259-267, 1972.

6. Von Winkle, W.A., J. Fitzgerald, W.M. Carey, and H.P. Bakewell, "Hydrodynamic Noise Surface Compliance," Naval Underwater Systems Center, Newport, R.I., Technical Document 6607, September 1982.

7. Corcos, G.M., "Resolution of Pressure in Turbulence," J. Acoust. Soc. Am., Vol. 35, pp 192-199, 1963.

8. Chase, D.M., "Modeling the wavevector-Frequency spectrum of Turbulent Boundary Layer Wall Pressure," J. Sound Vib., Vol. 70, pp 27-67, 1980.

9. Martini, K., P. Leehey, and M. Moeller, "Comparison of Techniques to Measure the Low Wavenumber Wall Pressure Spectrum," Acoustics and Vibrations Laboratory, M.I.T., Cambridge, Mass., Report 92828-1, August 1984.

10. Schewe, G., "On the Structure and Resolution of Wall-Pressure Fluctuations Associated with Turbulent Boundary-Layer Flow," J. Fluid Mech., Vol. 134, pp 311-328, 1983.

11. Willmarth, W.W., "Pressure Fluctuations Beneath Turbulent Boundary Layers," Annual Review of Fluid Mechanics, Vol. 7, pp 13-38, 1975.

12. Ash, R.L., and M.R. Khorrami, "Simulation of Turbulent Wall Pressure for Flexible Surface Response Studies," presented at the AIAA 21st Aerospace Sciences Meeting, Reno Nevada, Jan 10-13, AIAA Paper No. 83-0292, 1983.

13. Khorrami, M.R., "Effect of Transducer Size on the Statistical Properties of a Simulated Turbulent Wall Pressure Field," Master's Thesis, Mechanical Engineering and Mechanics Department, Old Dominion University, May 1983.

14. Bull, M.K., "Wall Pressure Fluctuations Associated with Sub-Sonic Turbulent Boundary Layer Flow," J. Fluid Mech., Vol. 28, pp 719-754, 1967.

15. Buckingham, A.C., R. C. Chun, R.L. Ash, and M.R. Khorrami, "Compliant Material Coating Response to a Turbulent Boundary Layer," presented at the AIAA/ASME Paper 82-1027, 1982.

16. Offen, G.R., and S.J. Kline, "Experiments on the Velocity Characteristics of 'Bursts' and on the Interaction Between the Inner and Outer Regions of a Turbulent Boundary Layer Flow," Thermosciences Division, Mechanical Engineering Dept., Stanford University, Report No. MD-31, 1973.

17. Willmarth, W.W., and C.E. Wooldridge, "Measurements of the Fluctuating Pressure at the Wall Beneath a Thick Turbulent Boundary Layer," J. Fluid Mech., Vol. 19, pp 187-210, 1962.

18. Bull, M.K., and Thomas, A.S.W., "High Frequency Wall Pressure Fluctuations in Turbulent Boundary Layers," Phys. Fluids, Vol. 19, pp 597-599, 1976.

19. Blake, W.K., "Turbulent Boundary Layer Wall Pressure Fluctuations on Smooth and Rough Walls," J. Fluid Mech., Vol. 44, pp 637-660, 1970.

20. Willmarth, W.W., and Roos, F.W., "Resolution and Structure of the Wall Pressure Field Beneath a Turbulent Boundary Layer," J. Fluid Mech., Vol. 28, pp 719-754, 1967.

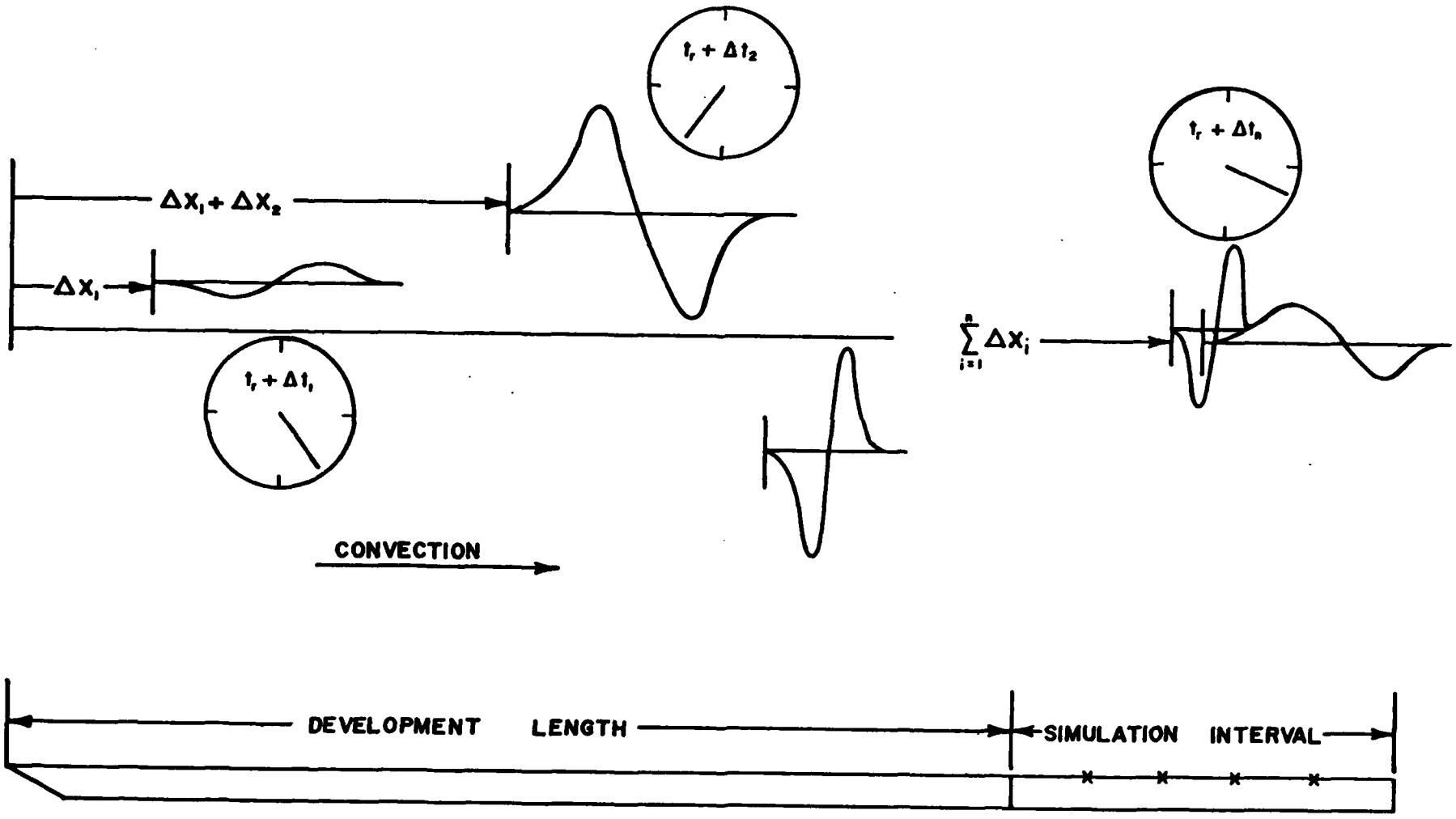

Figure 1. Representation of simulated pressure events during a single sweep.

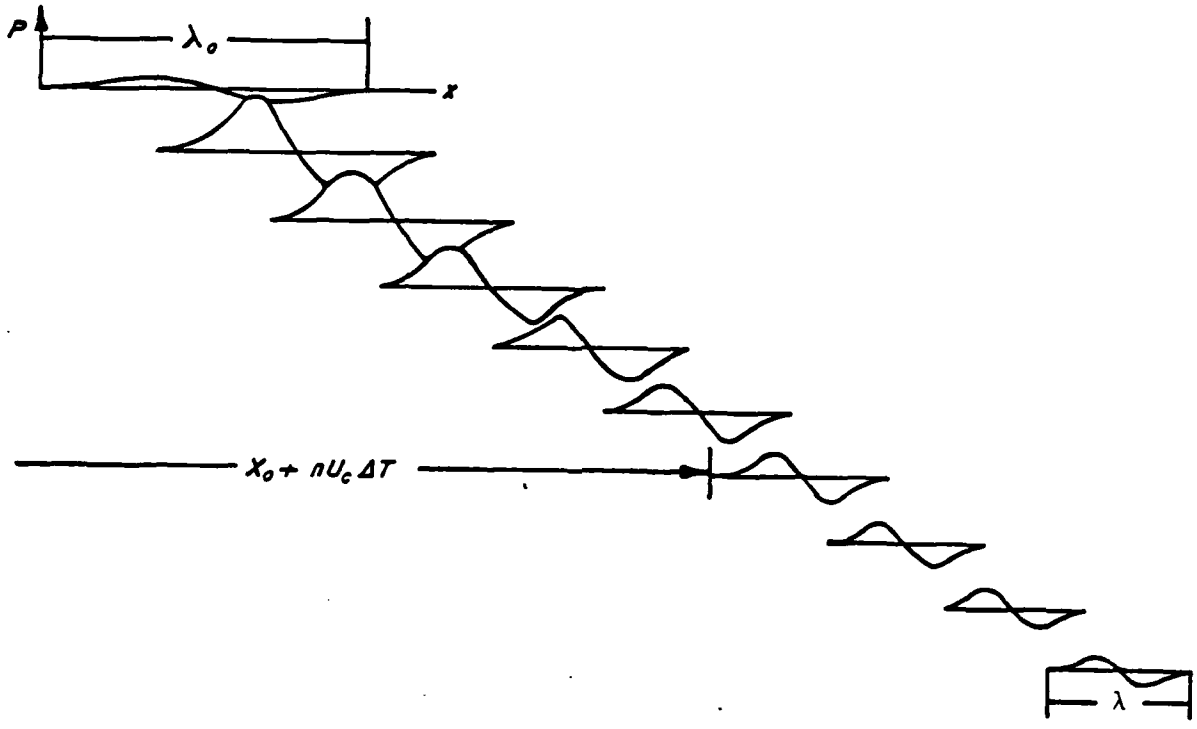

Figure 2. Variation of the amplitude and wavelength of a typical simulated pressure event as it is convected downstream.

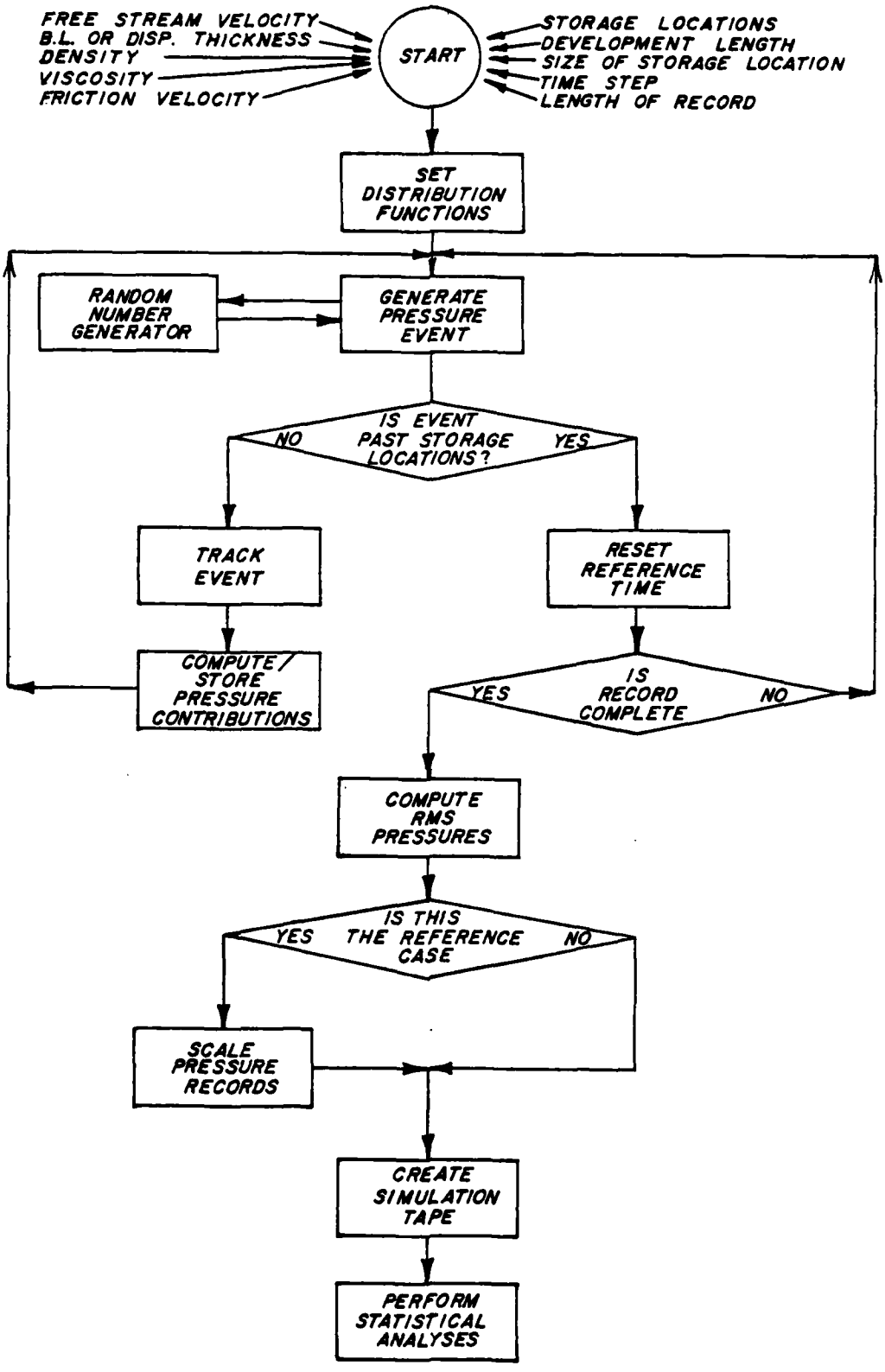

Figure 3. Flow chart representing the program for simulating P(x,t).

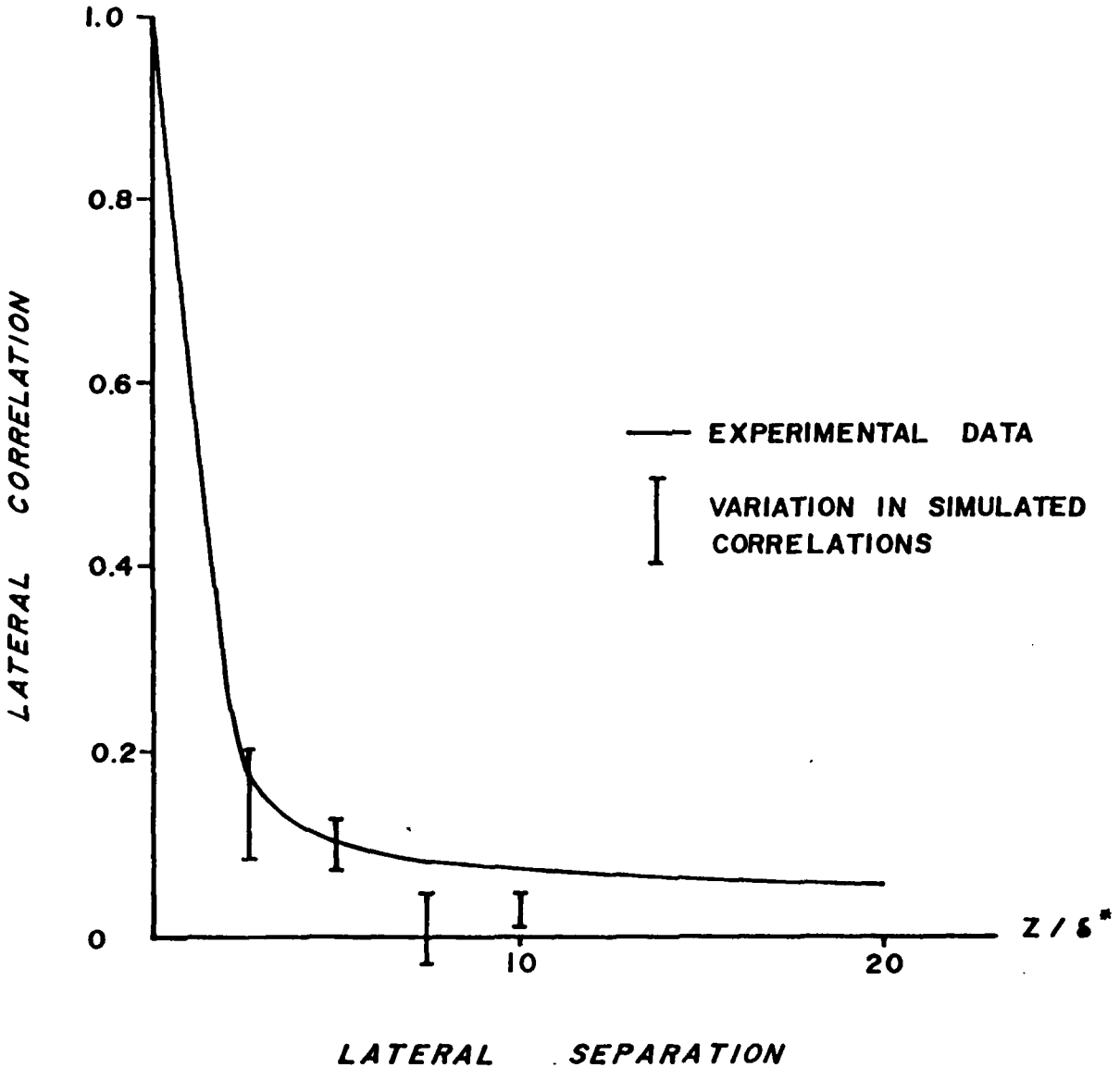

Figure 4. Comparison of lateral correlations from simulated P(x,z,t) and the experimental data from references 14 and 17.

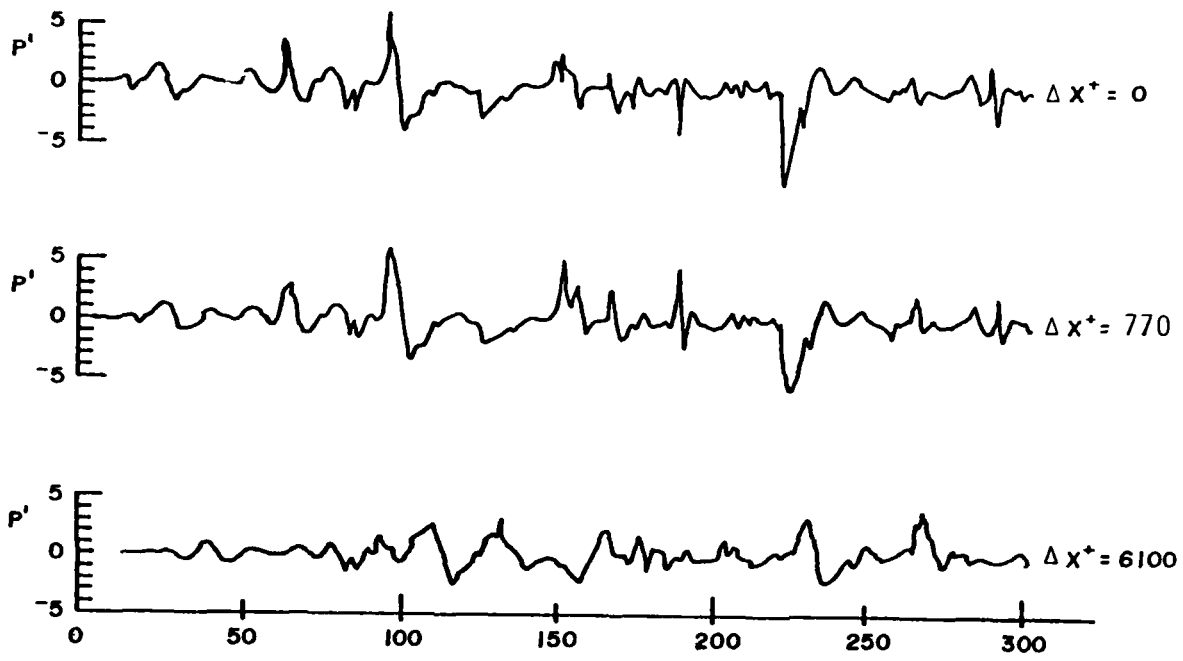

Figure 5. Simulated pressure histories for a reference location ($\Delta x^+ = 0$) and two downstream locations ($\Delta x^+ = 770$ and $\Delta x^+ = 6100$).

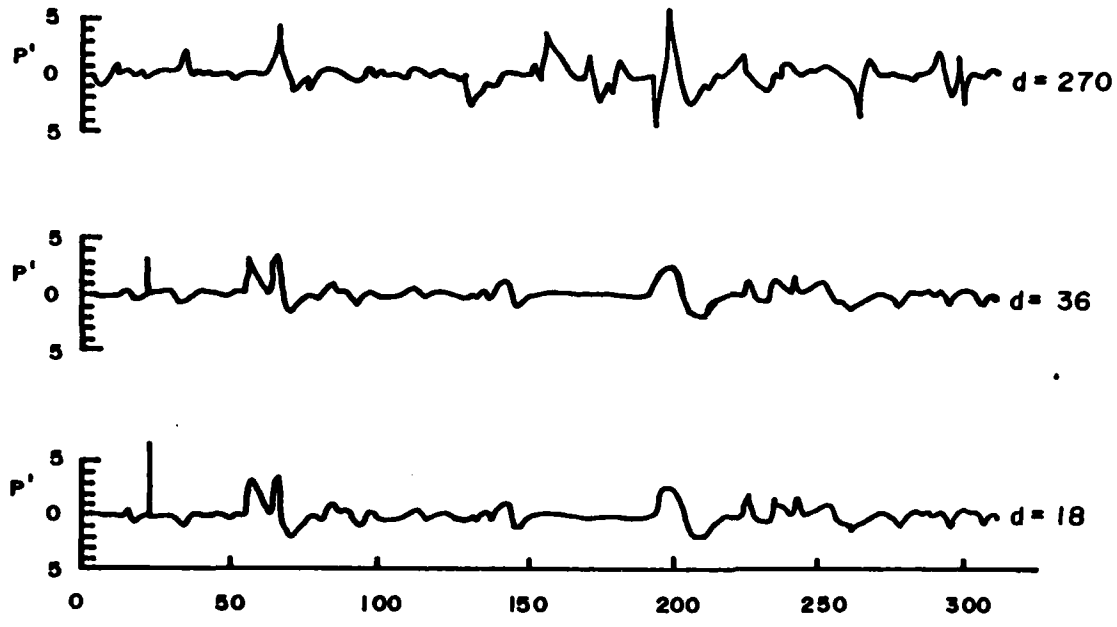

Figure 6. Influence of the size of the measurement area on the indicated pressure signal for identical (Px,t) histories.

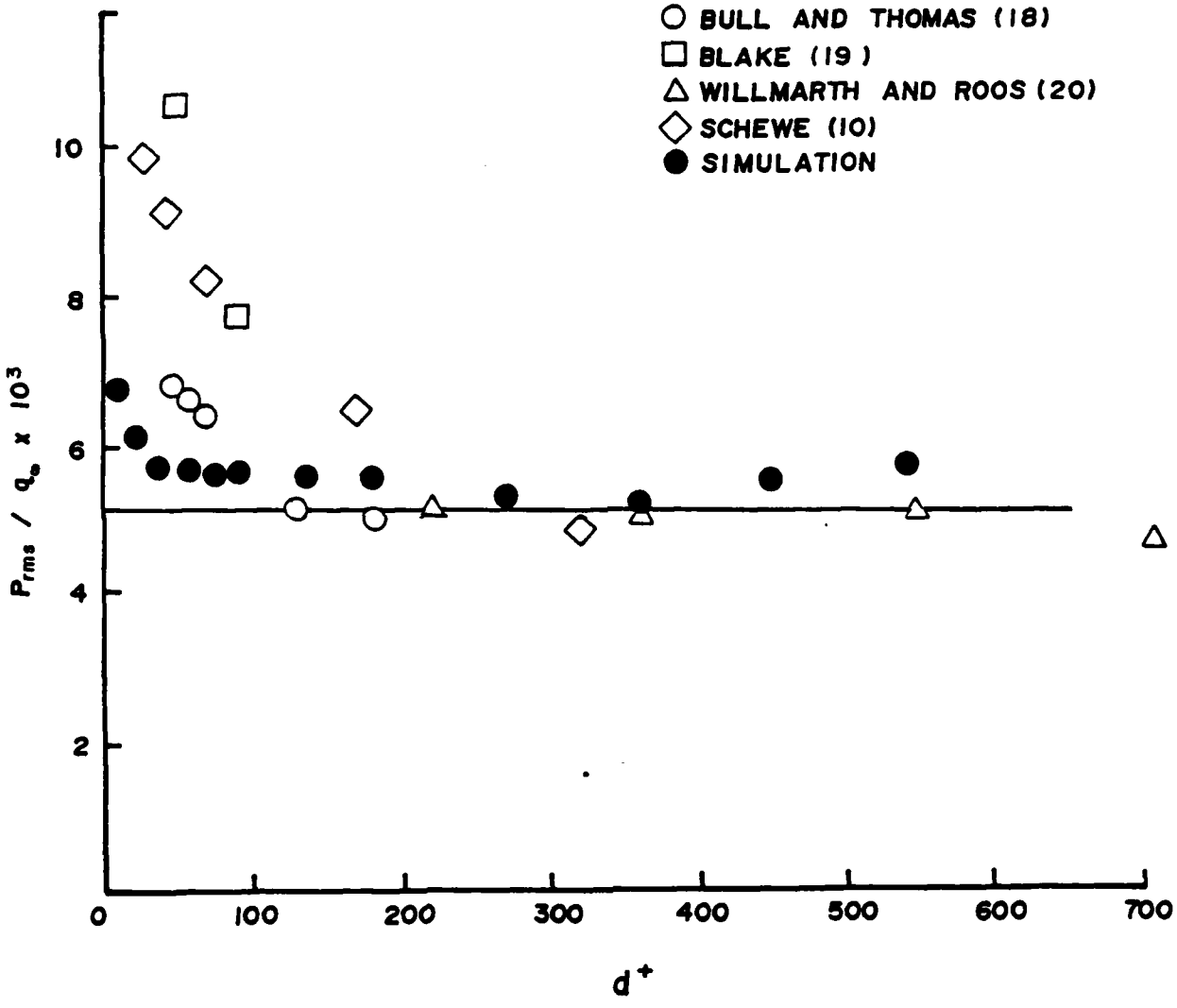

Figure 7. Influence of measurement area on root mean square pressure. Comparison between simulated data and experimental measurements.

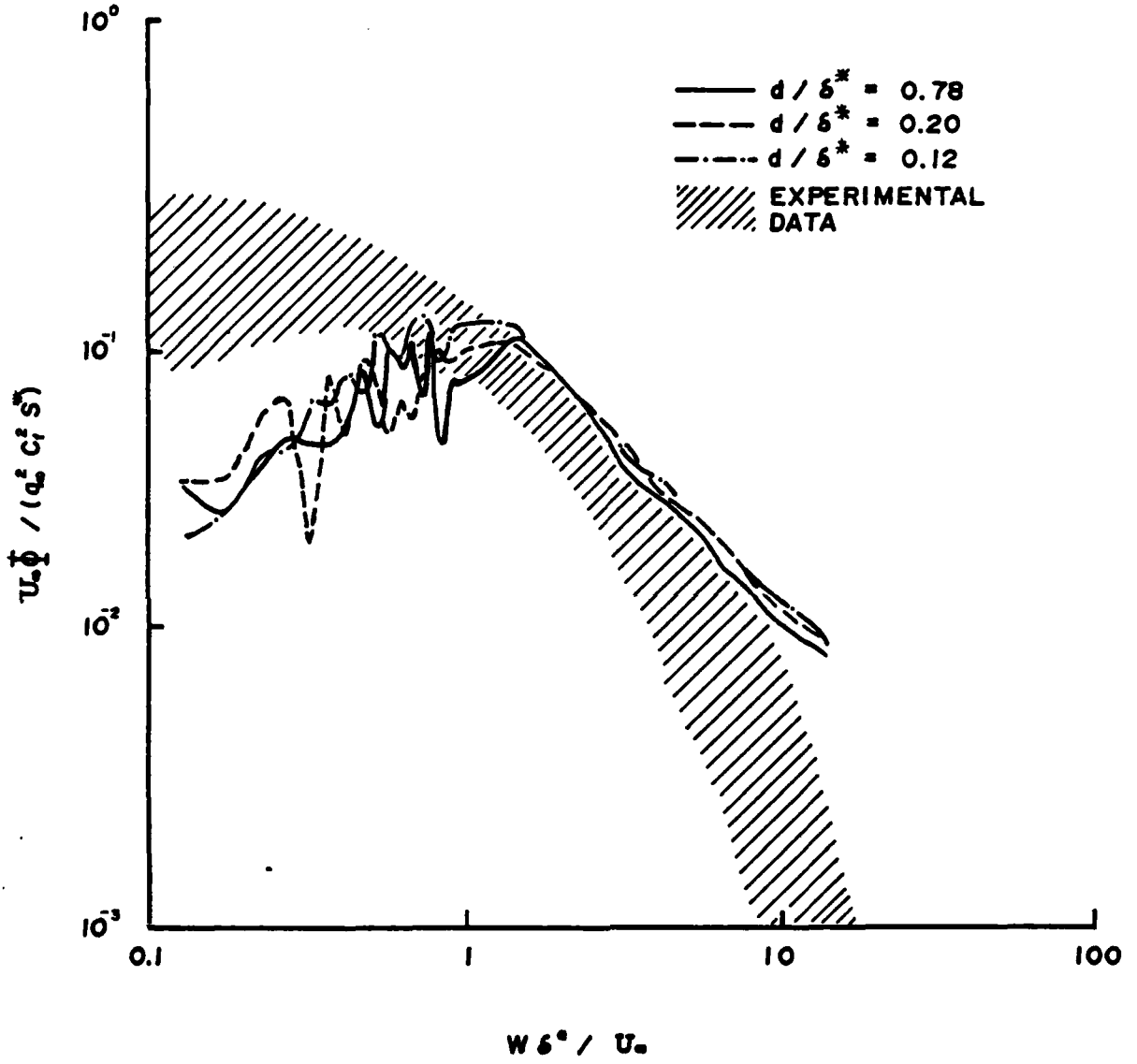

Figure 8. Influence of measurement area on power spectra for identical pressure histories.

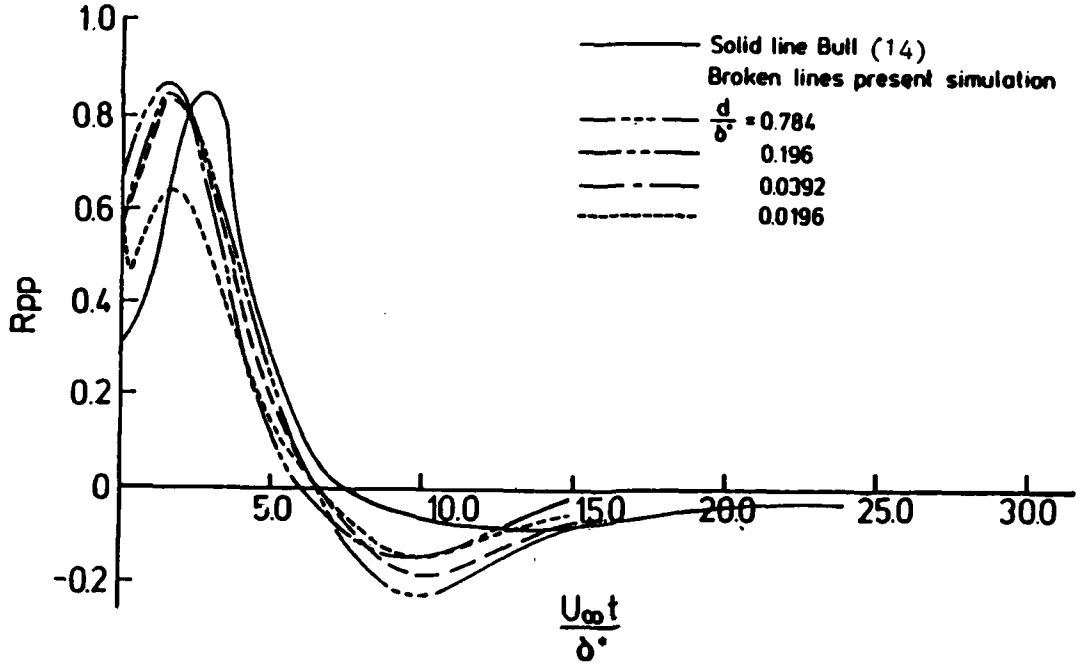

9a Variation of two-point correlations with measurement area $\Delta x/\delta^* = 1.7$ or $\Delta x^+ = 770$.

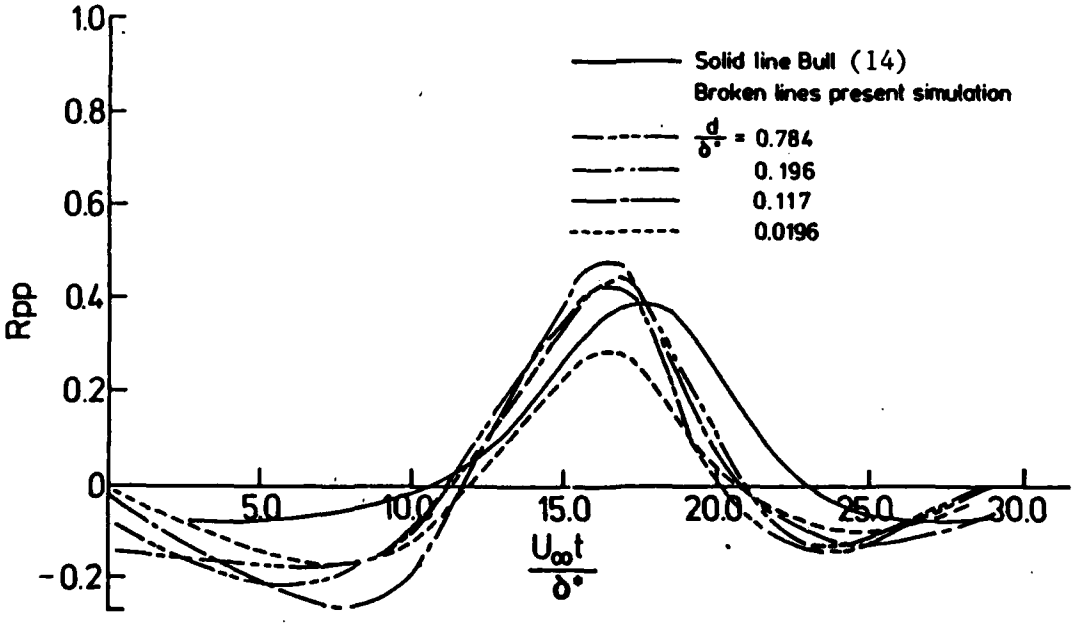

9b Variation of two-point correlations with measurement area $\Delta x/\delta^* = 13.4$ or $\Delta x^+ = 6100$.

Figure 9.

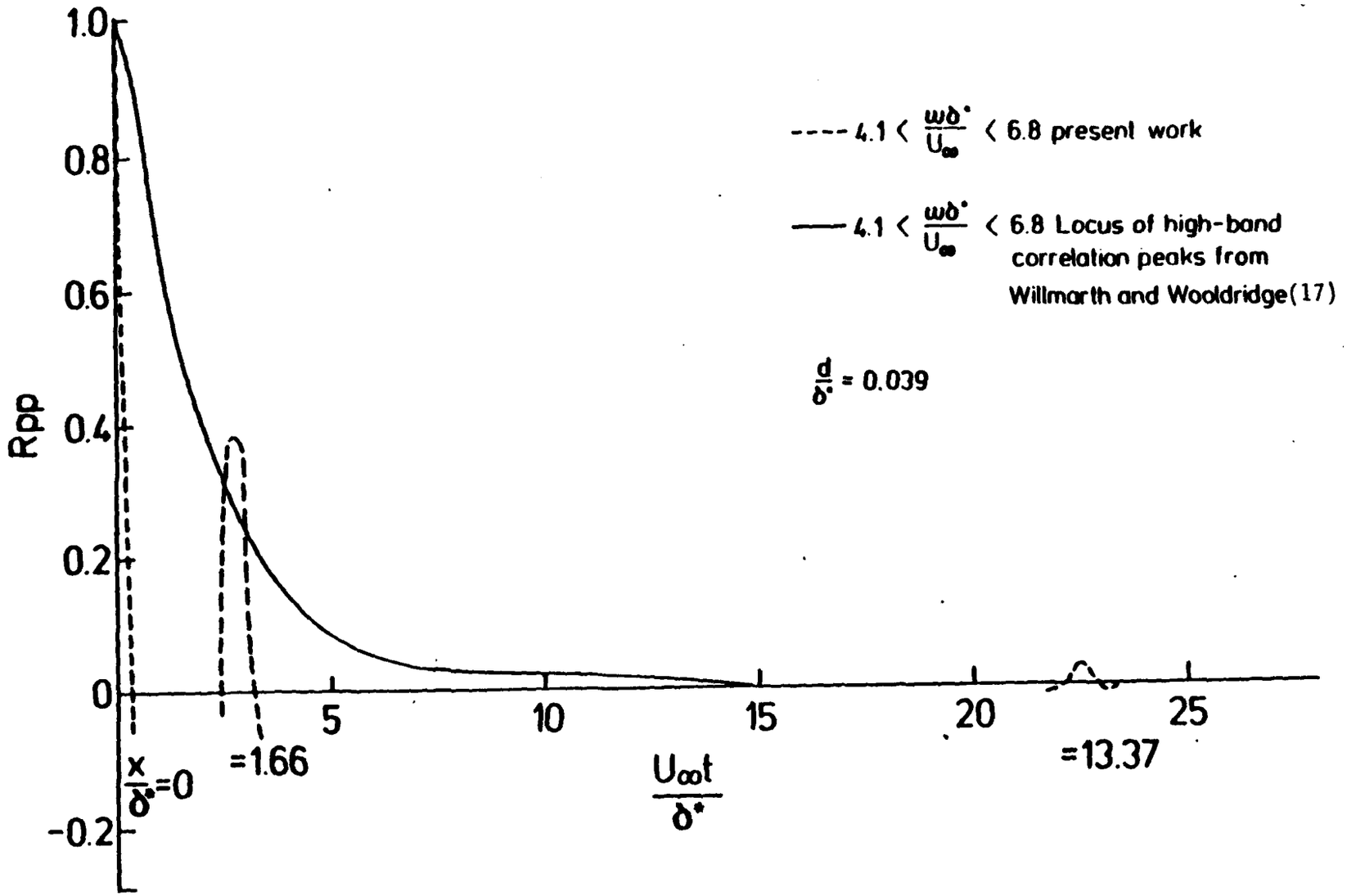

Figure 10. Comparison of filtered two-point correlations with experimental data. High frequency case.

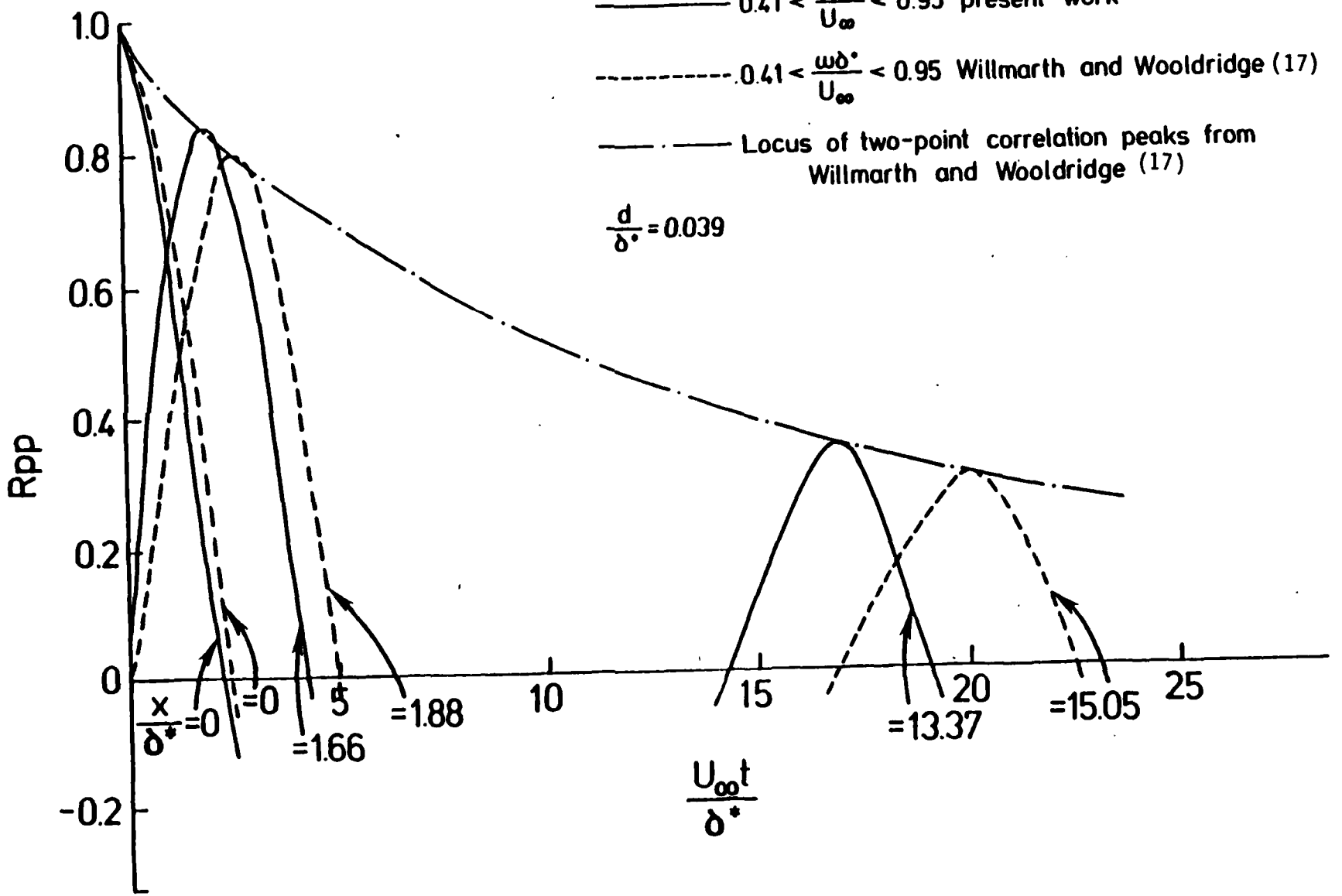

Figure 11. Comparison of filtered two-point correlations with experimental data. Low frequency case.

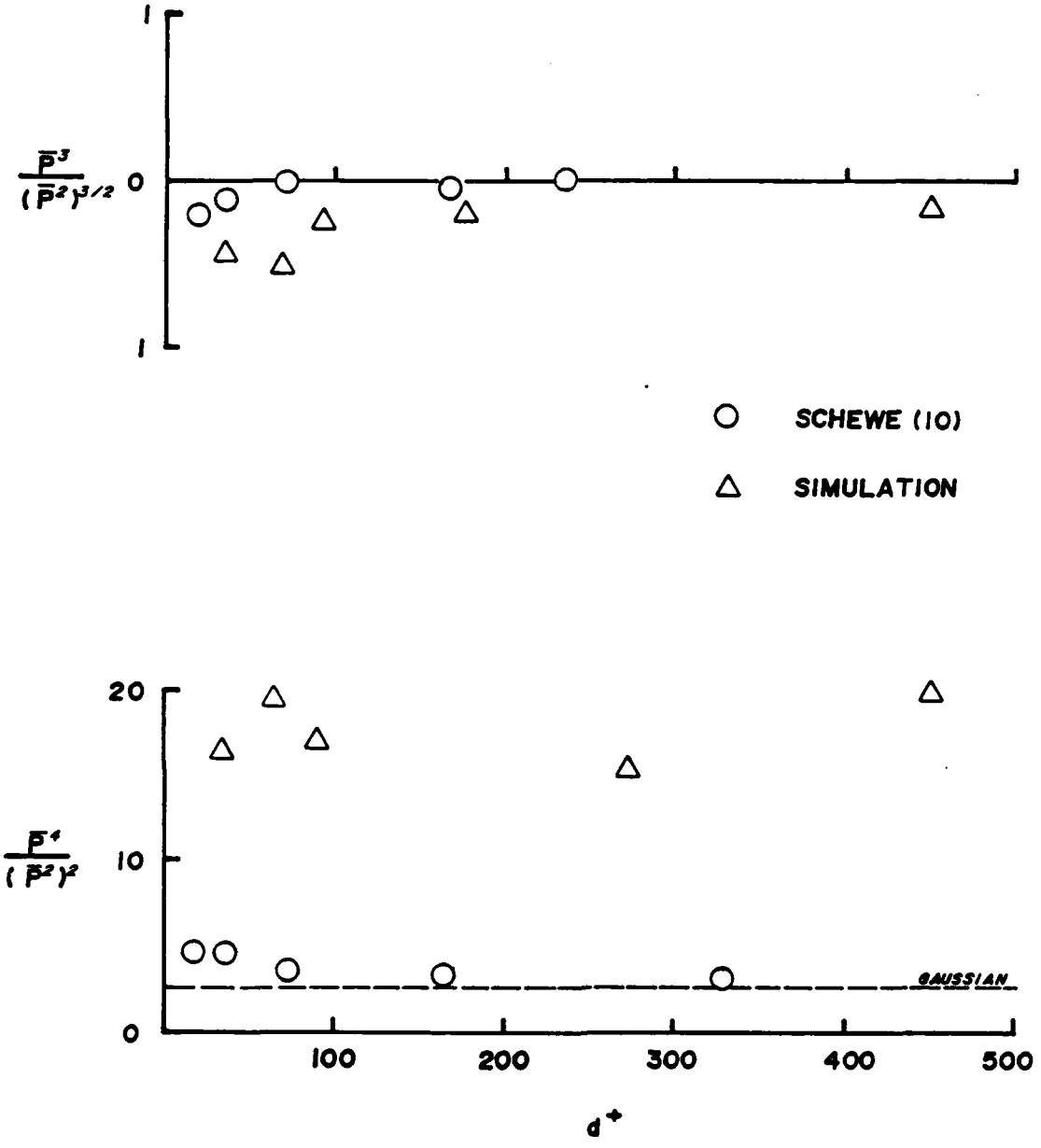

Figure 12. Comparison of the variation of skewness and flatness of simulated and measured wall pressure data.

END

FILMED

11-85

DTIC